IOP Conf. Series: Materials Science and Engineering **317** (2018) 012011 doi:10.1088/1757-899X/317/1/012011

Experiment Analysis and Modelling of Compaction Behaviour of Ag60Cu30Sn10 Mixed Metal Powders

Mengcheng Zhou[1], Shangyu Huang[1, 2, *], Wei Liu[1], Yu Lei[1] and Shiwei Yan[1]

[1]School of Materials Science and Engineering, Wuhan University of Technology, Wu Han 430070, China
[2]State Key Laboratory of Materials Processing and Die & Mould Technology, Huazhong University of Science and Technology, Wu Han 430070, China

Abstract. A novel process method combines powder compaction and sintering was employed to fabricate thin sheets of cadmium-free silver based filler metals, the compaction densification behaviour of Ag60Cu30Sn10 mixed metal powders was investigated experimentally. Based on the equivalent density method, the density-dependent Drucker-Prager Cap (DPC) model was introduced to model the powder compaction behaviour. Various experiment procedures were completed to determine the model parameters. The friction coefficients in lubricated and unlubricated die were experimentally determined. The determined material parameters were validated by experiments and numerical simulation of powder compaction process using a user subroutine (USDFLD) in ABAQUS/Standard. The good agreement between the simulated and experimental results indicates that the determined model parameters are able to describe the compaction behaviour of the multicomponent mixed metal powders, which can be further used for process optimization simulations.

1. Introduction

Due to the bad plastic workability, cadmium-free silver based brazing filler metals with high proportions of additional elements such as Zn, Sn, In, Ga, are too brittle to be made into thin sheets using conventional manufacturing processes [1, 2]. Recently, a novel process method that combines powder compaction and sintering was employed to fabricate thin sheets of the brittle and fragile cadmium-free silver based filler metals [3, 4]. The green powder compact is produced by cold die compaction of mixed metal powders and then undergoes a sintering process to attain the final thin sheets of filler metals with the desired properties. Since the any defects, cracks and density inhomogeneity generated at compaction stages will persist throughout the sintering process. Thus the properties of the filler metal sheet significantly depend on the quality of green compact which was related to the powder behaviour during compaction process. Therefore, it is of practical significance to investigate the compaction behaviour of mixed metal powders. In this paper, green compacts of filler metals Ag60Cu30Sn10 were fabricated, and the compaction behaviour of the mixed metal powders were investigated.

The finite element modelling (FEM) is an effective approach to investigate the powder behaviour considering the efficiency and cost. Based on simulations, the whole powder compaction process is simulated, and the powder densification behaviours, such as the distributions of stress and density, can be analyzed and predicted. In addition, the process parameters and tooling design optimization could be realized. While a proper constitutive model is vital for modelling the powder compaction process with continuum mechanics. So far, researches on metal powder compaction were mainly focused on densification of pure powders due to the complexity in densification of mixed powders [5]. To

describe the metal powder compaction behaviour, the ‘‘classical elastoplasticity’’ models were frequently employed, such as Kuhn [6], Green [7], Shima-Oyane [8] models. These models were expanded from the classical von-Mises model, which were generally proposed from uniaxial compression tests of sintered powder compacts. But they fail to capture the shearing phenomenon in powder compact which is significantly important during unloading and ejection process and are not suitable for describing the early stage of compaction [9, 10]. Moreover, most of these models were proposed for pure powder. To model the compaction behaviours of mixed metal powders, mixed yield functions were proposed by Kim [5, 11] with various mixing rules of soft and hard powders. Han [12] used the Voigt mixed-mode model to determine the yield strength and elastic parameters of the Fe and Al composite powders in simulations of the single action die compaction process. However, these models are too complicated and not applicable for multicomponent mixed metal powders in this paper. Since the densification behaviour of mixed metal powders and soil materials have many similarities, such as both of them are mixtures of particles with different mechanical features, material properties varied with densities. Meanwhile, the “soil mechanics” model, modified Drucker-Prager Cap (DPC) model, has been frequently employed to simulate the metal powder compaction [13, 14]. Thus, the modified DPC model was introduced to characterize the densification behaviour of mixed metal powders [3].

In this work, the compaction densification behaviour of Ag60Cu30Sn10 mixed metal powder was experimentally investigated. The density-dependent modified DPC plasticity model as well as a linear elasticity law was employed to model the powder densification behaviour. The model parameters and friction coefficients between the powders and die wall were determined experimentally. Validation experiments and finite element modelling of powder compaction process with a user subroutine (USDFLD) in ABAQUS/Standard were carried out to validate the obtained model parameters.

2. Constitutive model

The modified DPC[15] model employed in this work is a continuum mechanics model as shown in figure 1. The model assumes that the material is isotropic and its yield surface consists of three segments: a shear failure surface (F_s), a cap yield surface (F_c), and a transition region (F_t). The yield locus and plastic flow potential are dependent on the hydrostatic pressure stress p and the Mises equivalent stress q. The equations of the three surfaces are expressed as

$$F_s = q - p\tan\beta - d = 0 \tag{1}$$

$$F_c = \sqrt{\left(p - p_a\right)^2 + \left(\frac{Rq}{1+\alpha-\alpha/\cos\beta}\right)^2} - Rd\left(d + p_a\tan\beta\right) = 0 \tag{2}$$

$$F_t = \sqrt{\left(p - p_a\right)^2 + \left[q - \left(1 - \frac{\alpha}{\cos\beta}\right)\left(d + p_a\tan\beta\right)\right]^2} - \alpha\left(d + p_a\tan\beta\right) = 0 \tag{3}$$

where d and β are the cohesion and friction angle, respectively. R and α are parameters controlling the shape of the cap surface and the transition yield surface. The variable α is typically between 0.01 and 0.05, and is set as 0.02 in this work. p_a is an evolution parameter. p_b is the hydrostatic compression yield stress which defines the position of the cap, and is generally expressed as a nonlinear function of volumetric plastic strain

To fully define the yield surface, five parameters are required: d, β, R, p_a and p_b. In addition, two elastic parameters, the Young’s modulus E and Poisson ratio υ, and friction coefficient μ, are required to describe the elastic behaviour of the powder material and the friction between the powders and die wall, respectively. The material parameters were determined experimentally as function of relative density and the calibration methods were described in our previous research [3].

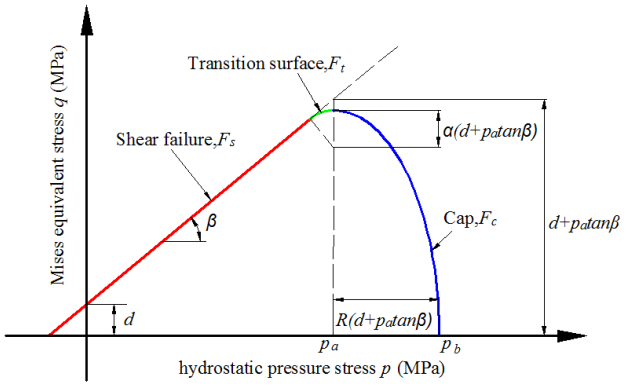

Figure 1. Yield surfaces of the modified Drucker-Prager Cap model[15].

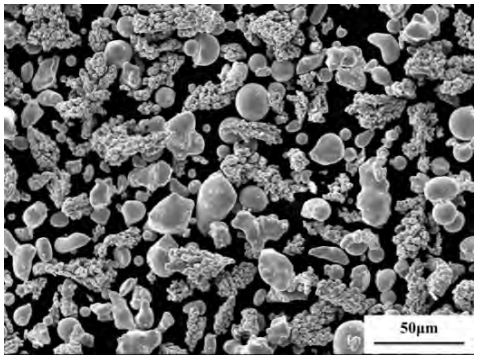

Figure 2. SEM images of the mixed metal powders.

3. Materials and experiments

3.1. Materials

The compositions and physical properties of Ag60Cu30Sn10 mixed powder were listed in table 1. To prepare the mixed metal powder, pure metal powders were weighed by an electronic balance according to their mass fractions. Subsequently, the powders were homogeneously mixed in vacuum using a planetary ball mill to prepare the mixed metal powders. The powder morphology was illustrated by SEM images as shown in figure 2. Based on the equivalent density method [3], the theoretical density of Ag60Cu30Sn10 was calculated as 9.582 g/cm^3.

Table 1. The composition and physical properties of two mixed metal powders.

Mixed metal Powders	Element components	Mass fraction (*wt%*)	Theoretical density (g/cm^3)	Particle sizes (μm)	Theoretical density (g/cm^3)
Ag60Cu30Sn10	Ag powder	60	10.53	1~45	9.582
	Cu powder	30	8.94	1~38	
	Sn powder	10	7.28	1~58	

3.2 Experiments

To investigate the densification behaviour of Ag60Cu30Sn10 mixed metal powders, series uniaxial compaction, diametrical compaction and instrumented die compaction tests were performed by using a WAW-600 (HUALONG, China) material testing system with a capacity of 600 KN. Uniaxial compaction and diametrical compaction tests were performed on samples with different relative densities to measure the axial compressive strength and radial tensile strength of compacts. In uniaxial compaction tests, the specimen diameter and height are 10 mm and 15 mm, respectively, and the compaction speed is 2 mm/min. In diametrical compaction tests, the compaction speed is 0.25 mm/min, the specimen diameter is 16mm and the specimen's thickness is ≤ 4mm. The instrumented die compaction tests were performed using the compaction apparatus as shown in figure 3. The strain-gauge measurement method [3] were employed to measure the radial stress during the powder compaction. The internal diameter, external diameter and height of the die are 10 mm, 20 mm and 50 mm, respectively. In the instrumented die compaction tests, an amount of 5.27 g Ag60Cu30Sn10 powder was manually poured into the die to achieve a uniform packing. The filling height was measured, and the initial filling relative density was calculated as 0.45. Loading and unloading were carried out by controlling the movement of the top punch with a constant load rate 0.2 KN/s to press the powder to different relative densities level, while the lower punch maintains stationary. The axial displacements of the load cylinder, the two axial forces and radial stress were recorded simultaneously. Two experiment cases are designed to characterize the friction between powders and die wall. Die

compaction tests with an unlubricated die, the inner die surface was cleaned by acetone and ethanol. Die compaction tests with a lubricated die, the inner die surface was lubricated using zinc stearate alcohol solution.

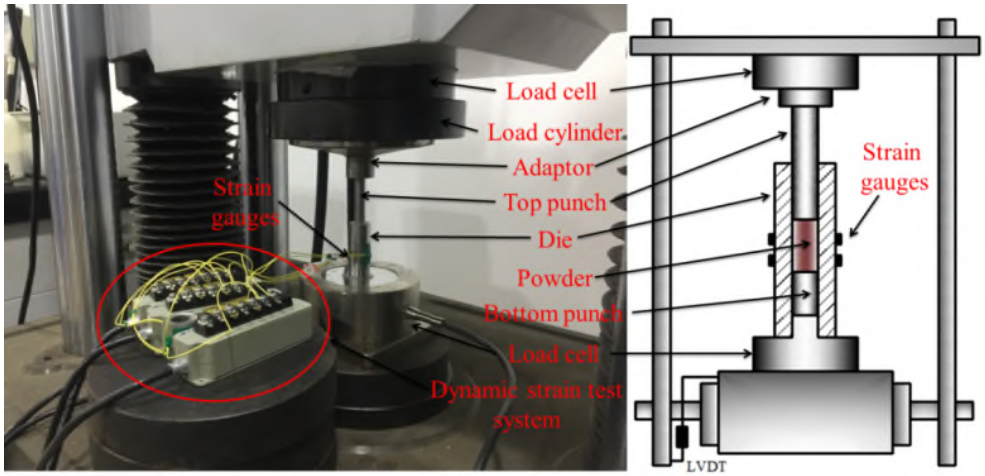

Figure 3. Schematic diagram of the instrumented die compaction test apparatus.

4. Results and discussion

4.1. Determination of the material parameters

The axial compressive and radial tensile strengths of powder compacts were measured by the diametrical compression and uniaxial compression tests, from which the cohesion d and friction angle β were determined as functions of relative density shown in figure 4. The cap surface parameters R, p_a and p_b, elastic parameters E and υ, were determined by instrumented die compaction tests which were shown in figures 5 and 6. All the experimentally calibrated material parameters were accurately fitted and extrapolated to low initial relative density regimes (< 0.6) to model the powder compaction behaviour. The friction coefficients μ between powder and the die wall in lubricated/unlubricated die were determined using the Janssen-Walker theory [16] as shown in Figure 6 (c). It can be observed that in lubricated die compaction, μ increased with top punch pressure at low pressure regime (≤ 50MPa), and then decreased gradually. But at the high pressure regime (> 125MPa), μ almost maintained a constant value of 0.08. In unlubricated die compaction, μ increased with top punch pressure at low pressure regime (≤ 70MPa), and then almost kept a constant value of 0.19.

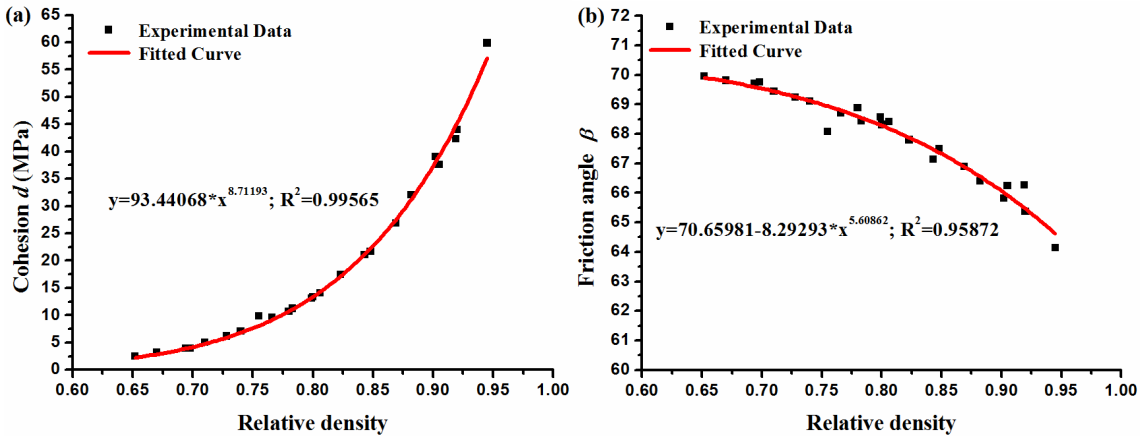

Figure 4. Shear failure surface parameters: (a) cohesion d, (b) friction angle β.

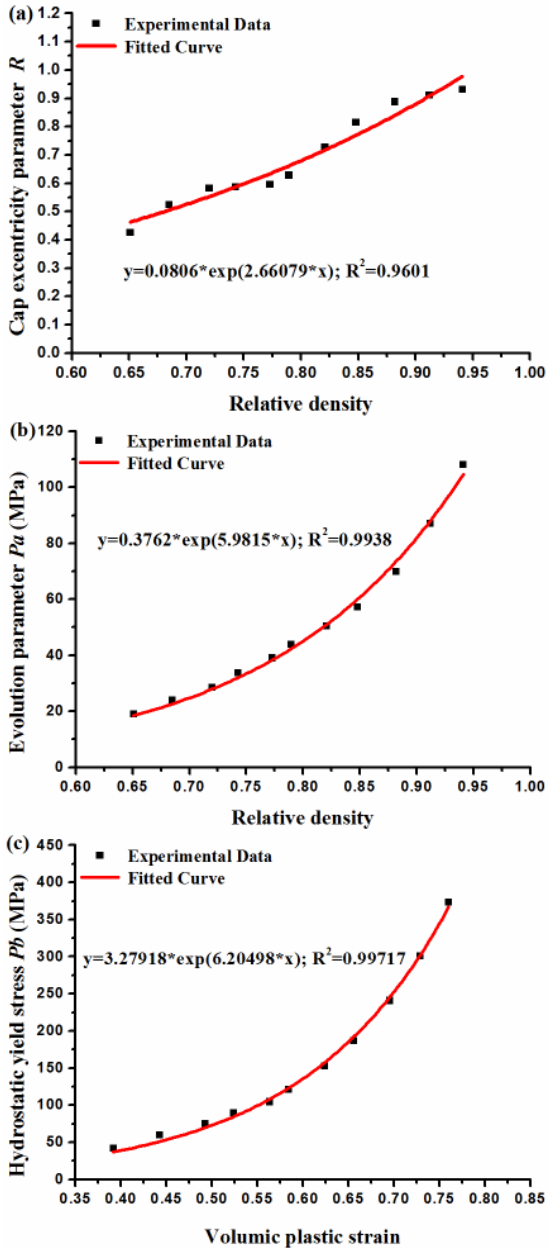

Figure 5. Cap surface parameters: (a) R, (b) p_a, (c) p_b.

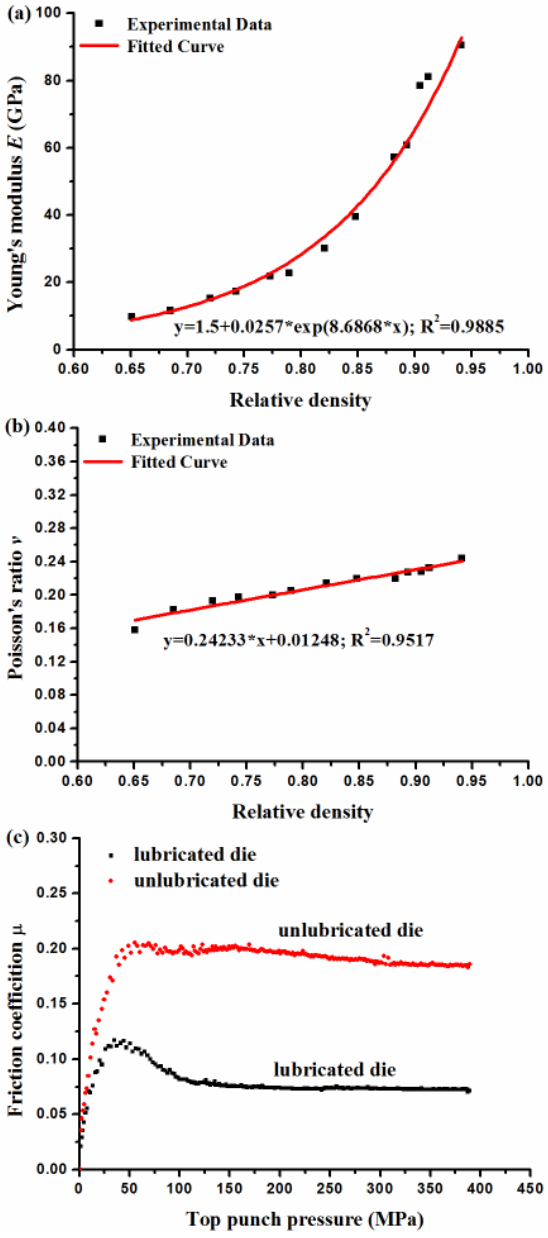

Figure 6. Elastic parameters and friction coefficient: (a) E, (b) υ, (c) μ.

4.2. Verification of the obtained material parameters

To validate the material parameters, validation experiments and simulations of powder compaction with lubricated/unlubricated die were performed. The characteristics of powder compacts prepared in the validation experiments, such as initial filling height H_0, the top punch displacement H_1, initial relative densityρ_0, final relative density ρ_1 and compaction pressure P, are presented in table 2. Since the geometry corresponding to the die compaction was axisymmetric, thus a quarter of 3D finite element model for the die compaction were analysed in ABAQUS/Standard. In simulations, the powder compact with a diameter of 10mm was modelled as a deformable continuum with C3D8R elements. The top/bottom punches and die were modelled as discrete rigid bodies with R3D4 elements. The friction coefficient between powder and tools were defined with a Coulomb friction model and were set as a constant value (table 2). In simulations, the top punch moved downward to press the powder during compaction and then moved upward during unloading, the bottom punch maintained

stationary. The determined elastic and plastic material parameters in section 4.1 were used in simulations. To characterize the evolution of material parameters with the relative density, a user subroutine USDFLD with a user-defined field for relative density was employed to update the elastic and plastic material parameters of powder during each time step.

Table 2. The characteristics of powder compacts in the validation experiments.

Compacts	m (g)	H_0 (mm)	H_1 (mm)	ρ_0	ρ_1 (experiment)	ρ_1 (simulation)	P (MPa) (experiment)	P (MPa) (simulation)
Lubricated die μ=0.08	5.286	15.55	8.04	0.452	0.912	0.916	389	389.8
Unlubricated die μ=0.19	5.27	15.2	7.49	0.461	0.893	0.884	389.2	393.1

The simulated results of relative density distributions in powder compacts after decompression were presented in figure 7. Due to the effect of the friction between the die and powders, the relative density is higher at the top corner contact with the die and lower in the bottom corner. It is also observed that because of the higher friction in unlubricated die, the density gradient is more remarkable. Figure 8 shows the comparison between the simulated and experimental loading-unloading curves. The simulated curves all matched well with the experimental data both in the loading and unloading steps. And the simulated results of the final relative density and compaction pressures were almost consisting with the experimental measurements as presented in table 2. The good agreement between the simulated and experimental results indicates that the experimentally determined density-dependent model parameters are able to precisely characterize the compaction behaviour of Ag60Cu30Sn10 mixed metal powders, and can be further used for process optimization simulations.

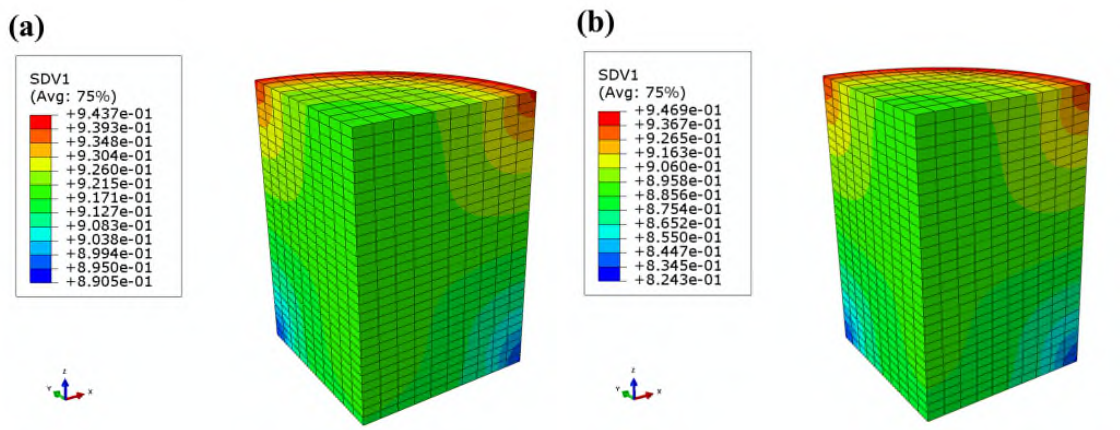

Figure 7. Relative density (SDV1) distribution in powder compact after decompression: (a) lubricated die, and (b) unlubricated die.

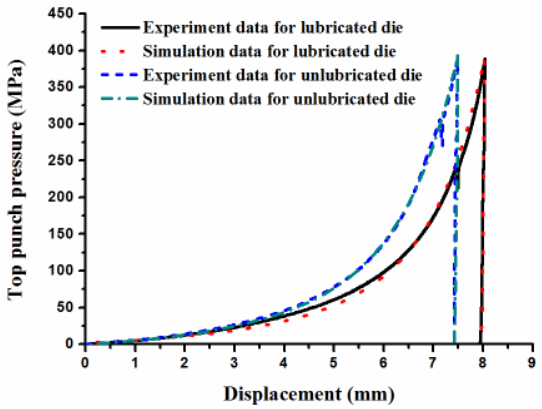

Figure 8. Comparison between the simulated and experimental loading-unloading curves.

5. Conclusions

The compaction densification behaviour of Ag60Cu30Sn10 mixed metal powders were investigated experimentally. Based on the equivalent density method, the density-dependent modified DPC model was employed to model the powder compaction behaviour. All the elastic and plastic material parameters were experimentally identified and were validated by validation experiments and finite element simulations of powder compaction process in ABAQUS/Standard with a user subroutine (USDFLD). The good agreement between the simulated and experimental results indicates that the determined model parameters can describe the mixed metal powder compaction behaviour, and can be further used for process optimization simulations.

Acknowledgments

This work was supported by National Natural Science Foundation of China (No.51475345), the Open Fund Project of State Key Laboratory of Materials Processing and Die & Mould Technology, Huazhong University of Science and Technology (No. P2015-01).

References

[1] Lai Z, Xue S, Lu F, et al. 2009 *China Weld* **18** 33-8.
[2] Weise W, Voelcker A, Kaufmann D, et al. 1996 *Cadmium-free silver alloy brazing solder, method of using said solder, and metal articles brazed with said solder*: US US5531962.
[3] Zhou M, Huang S, Hu J, et al. 2017 *Powder Technol.* **305** 183-96.
[4] Andrieux J, Dezellus O, Bosselet F, et al. 2008 *J. Phase Equilibria Diffus.* **29**1 56-62.
[5] Kim K T, Cho J H 2001 *Int. J. Mech. Sci.* **43** 2929-46.
[6] Kuhn H A, Downey C L 1971 *Int. J. Powder Metall.* **7** 15-25.
[7] Green R J 1972 *Int. J. Mech. Sci.* **14** 215-24.
[8] Shima S, Oyane M 1976 *Int. J. Mech. Sci.* **18** 285-91.
[9] Lee S C, Kim K T 2002 *Int. J. Mech. Sci.* **44** 1295-1308.
[10] Lee S C, Kim K T 2007 *Mater. Sci. Eng.* A **s445-446** 163-9.
[11] Cho J H, Kim K T 2001 *Int. J. Mech. Sci.* **43** 921-33.
[12] Han P, An X Z, Zhang Y X, et al. 2015 *J. Min. Metall.* **51** 163-71.
[13] Zadeh H K, Jeswiet J, Kim I Y 2013 *Int. J. Adv. Manuf. Technol.* **68** 1785-95.
[14] Zhou R, Zhang L H, et al. 2013 *Trans. Nonferrous Met. Soc. China.* **23** 2374-82.
[15] Han L H, Elliott J A, Bentham A C, et al. 2008 *Int. J. Solids Struct.* **45** 3088-106.
[16] Sinka I C, Cunningham J C, Zavaliangos A 2003 *Technol.* **133** 33-43.